Inorganic Chemistry

Article

pubs.acs.org/IC

Anomalous One-Electron Processes in the Chemistry of Uranium Nitrogen Multiple Bonds

Kimberly C. Mullane, Andrew J. Lewis, Haolin Yin, Patrick J. Carroll, and Eric J. Schelter*

P. Roy and Diana T. Vagelos Laboratories, Department of Chemistry, University of Pennsylvania, 231 South 34th Street, Philadelphia, Pennsylvania 19104, United States

Supporting Information

ABSTRACT: Novel reaction pathways are illustrated in the synthesis of uranium(IV), uranium(V), and uranium(VI) monoimido complexes. In contrast to the straightforward preparation of $U^{V}(=NSiMe_3)[N(SiMe_3)_2]_3$ (**1**), the synthesis of a uranium(V) tritylimido complex, $U^{V}(=NCPh_3)[N(SiMe_3)_2]_3$ (**4**), from $U^{III}[N(SiMe_3)_2]_3$ and Ph_3CN_3 was found to proceed through multiple one-electron steps. Whereas the oxidation of **1** with copper(II) salts produced the uranium(VI) monoimido complexes $U^{VI}(=NSiMe_3)X[N(SiMe_3)_2]_3$ (X = Cl, Br), the reaction of **4** with $CuBr_2$ undergoes sterically induced reduction to form the uranium(VI) monoimido complex $U^{VI}(=NCPh_3)Br_2[N(SiMe_3)_2]_2$, demonstrating a striking difference in reactivity based on imido substituent. The facile reduction of compounds **1** and **4** with KC_8 allowed for the synthesis of the uranium(IV) monoimido derivatives, $K[U^{IV}(=NSiMe_3)[N(SiMe_3)_2]_3]$ (**1-K**) and $K[U^{IV}(=NCPh_3)[N(SiMe_3)_2]_3]$ (**4-K**), respectively. In contrast, an analogous uranium(IV) monoimido complex, $K[U^{IV}(=NPh^F)[N(SiMe_3)Ph^F]]$, Ph^F = -pentafluorophenyl (**6**), was prepared through a loss of $N(SiMe_3)_2Ph^F$ concomitant with one-electron oxidation of a uranium(III) center. The uranium(IV) monoimido complexes were found to be reactive toward electrophiles, demonstrating N−C and N−Si single bond formation. One-electron reduction of nitrite provided a route to the uranium(VI) oxo/imido complex, $[Ph_4P][U^{VI}O(=NSiMe_3)[N(SiMe_3)_2]_3]$. The energetics and electrochemical processes involved in the various oxidation reactions are discussed. Finally, comparison of the $U^{VI}(=NSiMe_3)X[N(SiMe_3)_2]_3$, X = Cl, Br, complexes with the previously reported $U^{VI}OX[N(SiMe_3)_2]_3$, X = Cl, Br, complexes suggested that the donor strength of the trimethylsilylimido ligand is comparable to the oxo ligand.

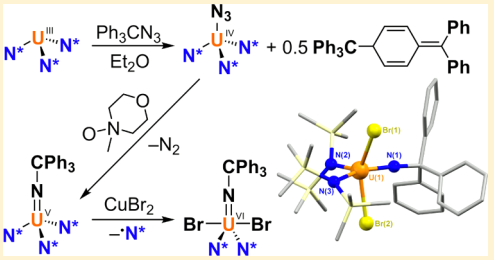

INTRODUCTION

Uranium-ligand multiple bonding is a topic of significant current interest,[1,2] with landmark recent discoveries in uranium−nitrogen multiple bonding including the isolation of the first example of a molecular uranium-nitride.[3−6] There are now a number of examples of high valent uranium bis(imido) complexes,[7−23] and several examples of uranium(VI) oxo/imido complexes.[13,24] The synthesis of uranium(IV) monoimido complexes has been successful with a variety of supporting ligands,[24−29] whereas uranium(VI) monoimido complexes are limited to two structurally related examples, $U^{VI}(=NR)F[N(SiMe_3)_2]_3$ (R = $-SiMe_3$, Ph).[30]

As part of our continuing studies of the inverse trans influence (ITI) in high valent uranium complexes with axial symmetry,[31−33] we demonstrated that reactive uranium(VI)−carbon bonds could be stabilized through coordination trans to a strong uranium-oxo multiple bond.[33] As a step toward engendering the stabilization of uranium-ligand bonds through ITI stabilization with the imido ligand, we sought to explore the influence of the imido substituent on the reactivity of the imido ligand itself, the relative donating ability of various imido ligands toward high valent uranium, and the extent of ITI stabilization relative to the oxo ligand.

The imido ligand is known to impart an ITI stabilization.[34] Uranium bis(imido) complexes exhibit electronic structures similar to that of uranyl, with a larger degree of 5f-ligand covalency in the U=NR bond relative to the U=O bond.[11] Recent work from Meyer and co-workers has alluded to the ability for the imido ligand to engage in varying degrees of ITI stabilization depending on the imido substituent.[35]

In this context, we turned our attention to monoimido complexes to explore their electronic structures with variable ligands trans to the imido group. Through these investigations, we observed several unexpected one-electron transfer processes. Synthetic pathways for formation of uranium imido linkages have primarily included the two-electron reduction of organoazides,[7,9,17,29,36−43] as well as deprotonation of primary amides.[3,13,21,26,38,44,45] In this work, we present the synthesis of a uranium−tritylimido complex, $U(=NCPh_3)[N(SiMe_3)_2]_3$, whose structure resembles a trityl-capped nitrido group, formed through sequential one-electron processes. We compare the one-electron reduction chemistry of $U(=NCPh_3)[N(SiMe_3)_2]_3$ with that of the complex $U(=NSiMe_3)[N(SiMe_3)_2]_3$, showing dramatically different outcomes. Further-

Received: May 16, 2014
Published: August 11, 2014

   dx.doi.org/10.1021/ic501149u | Inorg. Chem. 2014, 53, 9129−9139

more, the synthesis of a uranium(IV)-imido through one-electron oxidation of a uranium(III) center is presented, concomitant with silyl-group transfer. Comparison of the electronic structures and energetics of reactivity of the imido complexes is provided through DFT analysis.

RESULTS AND DISCUSSION

Synthesis of Uranium Mono−Imido Complexes. We recently described methods for the synthesis of uranium(VI) mono−oxo complexes, including the direct one electron oxidation of a uranium(V) oxo precursor, $U^{V}O[N(SiMe_3)_2]_3$, with Cu(II) salts.[32] Encouraged by the reported synthesis of $U^{VI}(=NSiMe_3)F[N(SiMe_3)_2]_3$ by Burns et al. using $AgPF_6$,[30] we attempted the analogous oxidation reactions of the uranium(V) imido precursor, $U^{V}(=NSiMe_3)[N(SiMe_3)_2]_3$ (**1**; Scheme 1), through divalent copper reagents. Complex **1**

Scheme 1. Synthesis of U^{V} and U^{VI} Mono−Imido Complexes

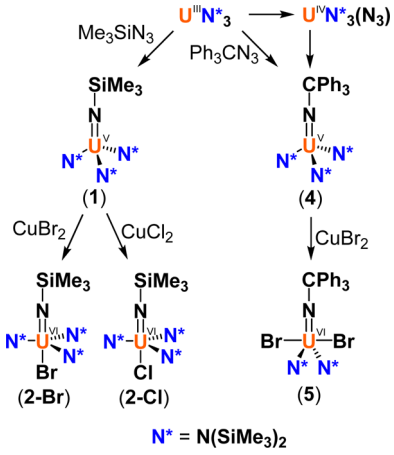

was conveniently obtained by the reported procedure, through the addition of Me_3SiN_3 to $U[N(SiMe_3)_2]_3$.[37,46] The addition of either $CuBr_2$ or $CuCl_2$ to **1** led to the immediate formation of the corresponding uranium(VI) products $U^{VI}(=NSiMe_3)Br[N(SiMe_3)_2]_3$ (**2-Br**) and $U^{VI}(=NSiMe_3)Cl[N(SiMe_3)_2]_3$ (**2-Cl**), respectively. Though the oxidation of uranium(IV) imido complexes with copper-based oxidants proved to be a broadly successful strategy in the synthesis of $(C_5Me_5)_2U^{V}X(=NAr)$ (Ar = 2,6-^{i}Pr$_2$C$_6$H$_3$, X = −F, −Cl, −Br, −I, −OTf, −SPh, −CCPh) complexes,[47−49] this reactivity has not been extended to the preparation of uranium(VI) monoimido complexes. The ^{1}H NMR spectra of **2-Br** and **2-Cl** both exhibited two resonances for the bis(trimethylsilylamide) ligands in a 1:1 ratio, with one very broad resonance and one sharp resonance. The difference in the peak widths was attributed to steric clash between the bulky $-SiMe_3$ groups of the imido and amide ligands causing hindered rotation.[30−33]

Having established the reactivity of the uranium(V) monoimido complex **1** toward copper oxidants, we turned to the one-electron reduction of nitrite, a protocol that we previously reported in the synthesis of uranium(VI) mono−oxo complexes.[32] Replacement of a uranium(IV)− or uranium(V)−halide bond with nitrite led to spontaneous formation of the uranium(V)− or uranium(VI)−oxo product through the loss of nitric oxide. Recent work from Cantat and co-workers showed that the use of $[Ph_4P][NO_2]$ rather than $NaNO_2$ or $AgNO_2$ allowed for installation of the nitrite ion into an open coordination site, rather than through displacement of a halide.[50] The addition of $[Ph_4P][NO_2]$ to **1** led to formation of the orange-red uranium(VI) oxo/imido complex $[Ph_4P][U^{VI}O(=NSiMe_3)[N(SiMe_3)_2]_3]$ (**2-O**), in 69% yield (Scheme 2). The two reported preparations of oxo/imido

Scheme 2. Synthesis of U^{VI} Oxo/Imido Complex 2-O

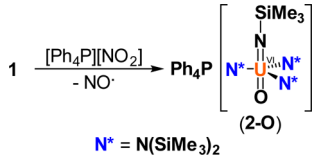

complexes were through hydrolysis of uranium(VI) bis(imido) complexes[13] and through oxygen atom transfer to uranium(IV) monoimido complexes.[24,38]

X-ray structural analysis of **2-Br**, **2-Cl**, and **2-O** (Figures 1 and 2) allowed for comparison of the bond metrics with the

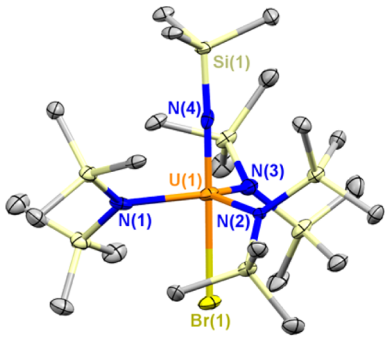

Figure 1. Thermal ellipsoid plot of **2-Br** at 30% probability. Bond lengths (Å) and angles (deg): U(1)−Br(1) 2.7675(11), U(1)−N(1) 2.222(10), U(1)−N(2) 2.191(9), U(1)−N(3) 2.215(10), U(1)−N(4) 1.907(9), Br(1)−U(1)−N(4) 179.5(2), U(1)−N(4)−Si(1) 177.2(5).

structurally related oxo-halides $U^{VI}OBr[N(SiMe_3)_2]_3$ (**3-Br**) and $U^{VI}OCl[N(SiMe_3)_2]_3$ (**3-Cl**),[32] as well as the uranyl complex $[Na(THF)_2][UO_2[N(SiMe_3)_2]_3]$ (**3-O**).[51] In each case, the **2-X** complex exhibited longer equatorial U−N bond lengths relative to the corresponding **3-X** complexes, indicative

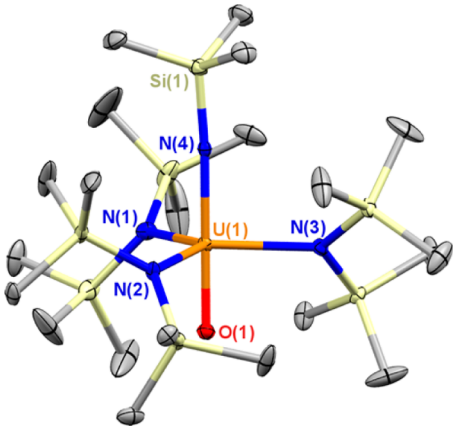

Figure 2. Thermal ellipsoid plot of **2-O** at 30% probability. Hydrogen atoms, disorder of the methyl substituents of the imido ligand, and the $[Ph_4P]^{+}$ ion are omitted for clarity. Bond lengths (Å) and angles (deg): U(1)−N(1) 2.348(3), U(1)−N(2) 2.347(3), U(1)−N(3) 2.346(3), U(1)−N(4) 1.980(3), U(1)−O(1) 1.805(2), O(1)−U(1)−N(4) 179.82(12), U(1)−N(4)−Si(1) 176.15(18).

dx.doi.org/10.1021/ic501149u | Inorg. Chem. 2014, 53, 9129−9139

of greater destabilization of the U−N bonds (Table 1). Though the differences in the bond lengths were small, they were well

Table 1. Experimental and Calculated Equatorial U−N Bond Lengths in the 2-X and 3-X Complexes (X = Br, Cl, O)

	U−N_{eq}	
	exptl.	calcd.
2-Br $U^{VI}(=NSiMe_3)Br(N^*)_3$[a]	2.209(11)	2.235
3-Br $U^{VI}OBr(N^*)_3$[a]	2.200(3)[b]	2.219[b]
2-Cl $U^{VI}(=NSiMe_3)Cl(N^*)_3$[a]	2.205(15)	2.235
3-Cl $U^{VI}OCl(N^*)_3$[a]	2.193(2)[b]	2.221[b]
2-O $[Ph_4P][U^{VI}(=NSiMe_3)O(N^*)_3]$[a]	2.347(4)	2.389
3-O $[Na(THF)_2][U^{VI}O_2(N^*)_3]$[a]	2.310(5)[c]	2.350[c]

[a]$N^* = N(SiMe_3)_2$. [b]From ref 32. [c]From ref 51.

reproduced in the calculated geometries (*vide infra*). Greater destabilization of the cis metal−ligand bonds relative to the strong trans-axial donor ligands is indicative of a more significant ITI,[33,52−55] suggesting, surprisingly, that the trimethylsilylimido donor ability is comparable to that of the oxo ligand.

Having established the straightforward oxidation chemistry of **1**, we sought to expand this reactivity to the potentially more chemically interesting triphenylmethyl (trityl) functional group. The trityl moiety functions as an effective protecting group in a variety of organic reactions,[56] and the cleavage of Ph_3C-X bonds is a useful pathway for the oxidative installation of new uranium−ligand bonds,[57−59] including a recent example of the formation of uranium−oxo and −sulfido multiple bonds.[60] In fact, the low-temperature reaction of Ph_3CN_3 with $U^{III}[N(SiMe_3)_2]_3$ is known to form the product of one-electron oxidation, $U^{IV}(N_3)[N(SiMe_3)_2]_3$ (Scheme 1), through loss of a trityl radical and formation of Gomberg's dimer.[46] Similarly, the reaction of $U^{III}(OAr)_3TACN$ with Me_3SiN_3 was reported to produce a mixture of both the uranium(V) monoimido through two-electron oxidation as well as the uranium(IV) azide through the loss of a trimethylsilyl radical and subsequent formation of hexamethyldisilazane.[58]

We found that formation of $U^{IV}(N_3)[N(SiMe_3)_2]_3$ through the low temperature addition of Ph_3CN_3 followed by the addition of *N*-methylmorpholine-*N*-oxide led to a color change to dark green and vigorous gas formation, to produce $U^{V}(=NCPh_3)[N(SiMe_3)_2]_3$ (**4**) in 93% yield. More conveniently, the room temperature addition of Ph_3CN_3 to $U^{III}[N(SiMe_3)_2]_3$ in Et_2O generated **4** directly. When this reaction was performed in pyridine at room temperature, only the uranium(IV) azide product was generated, and addition of *N*-methylmorpholine-*N*-oxide led to decomposition.

The X-ray structure of **4** revealed a C_3 symmetric, sterically congested structure (Figure 3). The U=N multiple bond distance was determined to be 1.959(5) Å, longer than that of **1** at 1.910(6) Å,[37] and the average U−N amido bonds were 2.264(3) Å, slightly shorter than those of **1** at 2.295(10).[37] The trityl group of **4** imparted a more sterically encumbered coordination environment at the coordination site trans to the imido ligand than that of **1**. The electronic absorption spectrum

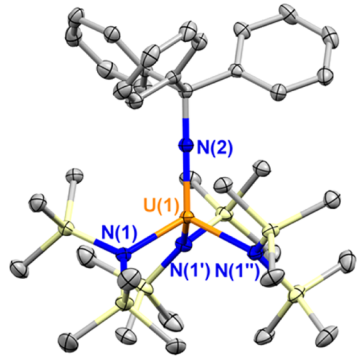

Figure 3. Thermal ellipsoid plot of **4** at 30% probability. Hydrogen atoms are omitted for clarity. Bond lengths (Å) and angles (deg): U(1)−N(1) 2.264(3), U(1)−N(2) 1.959(5), U(1)−N(1)−C(1) 180.00, N(1)−U(1)−N(2) 113.90(7).

of **4** showed broad absorbance throughout the visible region, and high intensity absorption in the UV attributed to $\pi \rightarrow \pi^*$ transitions within the trityl moiety (Figure S12). The near-IR spectrum of **4**, in the energy range of 5f → 5f transitions, showed poorly resolved low intensity features compared to the analogous spectrum of $U^{V}O[N(SiMe_3)_2]_3$,[61] which exhibited four sharp absorptions. Similar behavior has been observed in the comparison of the near-IR spectra of uranium(V)−oxo and −imido complexes previously.[62]

The (presumably) sterically congested environment in **4** caused the reactions with Cu(II) to proceed differently from those with **1** (Scheme 1). The addition of $CuBr_2$ in THF produced a brown product that appeared to be diamagnetic by ^{1}H NMR, with a curious 2:1 ratio of $-N(SiMe_3)_2$ to $=NCPh_3$ ligand protons, inferred from integration. X-ray structural analysis of a single crystal of the product grown from hexanes at −21 °C revealed the structure to be $U^{VI}Br_2(=NCPh_3)[N(SiMe_3)_2]_3$ (**5**). Elemental analysis supported the ^{1}H NMR assignment, though the X-ray data were of insufficient quality for complete refinement (Figure S2).

Isolation of **5** was achieved in 83% yield, discounting the possibility that it was a product of ligand redistribution. Additionally, no production of $[Cu[N(SiMe_3)_2]_2]_4$ was observed,[63] ruling out transmetalation. Formation of **5** implies the formal loss of the aminyl radical, $^{\bullet}N(SiMe_3)_2$.[64] We have previously observed a loss of aminyl radical in the formation of $U^{VI}O_2(THF)_2[N(SiMe_3)_2]_2$ from the reaction of $U^{VI}OCl[N(SiMe_3)_2]_3$ with $NaNO_2$, which was attributed to the strong thermodynamic driving force of uranyl formation as well as the absence of valence electrons on the $5f^0$ metal center.[32] Similarly, $U-N(SiMe_3)_2$ and $Ln-N(SiMe_3)_2$ bond homolysis has led to single-electron reduction of uranyl in the work of Arnold et al.,[65,66] also to form strong metal-oxo bonds. We were therefore surprised at the ability to install weaker bromide ligands, especially considering the relatively poorer stability of the aminyl fragment relative to the bromide radical. However, while this reaction proceeds cleanly in THF, no reaction was observed in toluene, a solvent less prone to hydrogen atom donation, implicating the need for hydrogen atom abstraction from the solvent to form free $HN(SiMe_3)_2$. We offer that the synthesis of **5** is best described as a sterically induced reduction, a process common among $(C_5Me_5)_3Ln$ and $(C_5Me_5)_3U$ complexes.[67]

Anomalous uranium monoimido formation through single-electron transfer was also observed with a modified ligand,

dx.doi.org/10.1021/ic501149u | Inorg. Chem. 2014, 53, 9129−9139

$[N(SiMe_3)Ph^F]^-$ (Ph^F = pentafluorophenyl). The electron-withdrawing $-Ph^F$ group evidently increases the electrophilicity of the $-SiMe_3$ group and induces facile silyl-migration upon coordination of metal cations, leading to the formation of imido species.[68,69] Treatment of $UI_3(THF)_4$ with 3 equiv of $KN(SiMe_3)Ph^F$ followed by crystallization from hexanes consistently produced light red crystals identified as $K[U^{IV}(=NPh^F)[N(SiMe_3)Ph^F]_3]$ (**6**) in 17% yield (Scheme 3). The side-product formed in this reaction was a tertiary amine, $N(SiMe_3)_2Ph^F$, which was assigned by comparison of the ^1H and ^{19}F NMR spectra with the known compound.[70] Thus, the formation of **6** is likely the result of elimination of $N(SiMe_3)_2Ph^F$ accompanied by one-electron oxidation of the metal center through disproportionation of a U^{III} intermediate.[71,72] Formation of a uranium−imido complex through loss of a trimethylsilyl moiety was observed in one previous instance, where treatment of $[U[N(SiMe_3)_2]_2Cl_2]_2$ with KC_8 led to isolation of $[U(=NSiMe_3)[N(SiMe_3)_2]_2(\mu\text{-Cl})]_2$ from a mixture of products.[73] Compound **6** was unstable in solution and thus was only isolated in poor yield. This instability is due to further reactions accompanied by a loss of $N(SiMe_3)_2Ph^F$ equivalents; in one instance, we were able to identify a uranium(V) bis(imido) side product through the addition of 18-crown-6, $[K(18\text{-crown-6})(THF)_2][U(=NPh^F)_2(THF)_2[N(SiMe_3)Ph^F]_2]$ (Figure S5), though the low yield of this product prevented full characterization.

Scheme 3. Synthesis of U^{IV} Mono−Imido Complex 6

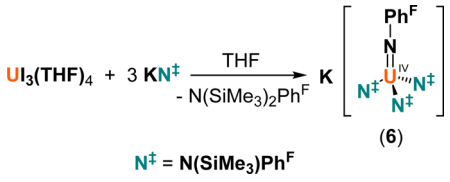

Reduction Chemistry and Reactivity. The accessibility of the 5-coordinate complexes **2-Cl**, **2-Br**, and **2-O** suggested that the coordination sphere in **1** was not completely saturated. We anticipated that a larger uranium(IV) ion in this coordination environment would prove susceptible to further reactivity. Treatment of **1** with excess KC_8 led to smooth conversion to the expected reduction product, $K[U(=NSiMe_3)[N(SiMe_3)_2]_3]$ (**1-K**), isolated as a pink solid in 87% yield (Scheme 4). The ^1H NMR spectrum of **1-K** exhibited a broad resonance at −7.9 ppm corresponding to the $-N(SiMe_3)_2$ ligands and a sharp resonance at 34.6 ppm corresponding to the $=NSiMe_3$ ligand. The electronic absorption spectrum of **1-K** in toluene supported the 4+ oxidation state assignment (Figure S13), with low intensity absorption in the visible region, and numerous features observed in the near-IR portion of the spectrum, typical of uranium(IV) complexes.[74,75] Treatment of **4** with excess KC_8 gave the analogous uranium(IV) compound, $K[U(=NCPh_3)[N(SiMe_3)_2]_3]$ (**4-K**), which crystallized as a pale orange solid in 50% yield. The ^1H NMR spectrum for **4-K** showed a broad resonance at −8.9 ppm corresponding to the $-N(SiMe_3)_2$ ligand protons, and three resonances at 41.1, 13.8, and 12.0 ppm corresponding to the aryl resonances from the $=NCPh_3$ group.

The X-ray crystal structure of **1-K** was obtained as the benzene-d_6 solvate following suspension of the complex in benzene-d_6, removal of the volatiles, and crystallization from pentane (Figure 4, top). The K^+ ion closely associated with the

Scheme 4. Synthesis of Uranium(IV) Mono−Imido Complexes and Reactivity toward Electrophiles

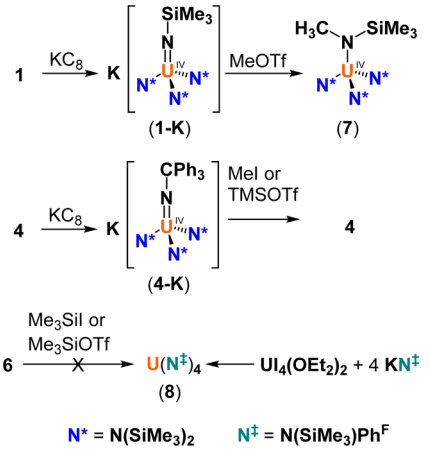

imido ligand at a K−N distance of 2.957(3) Å, analogous to the structure of the reported anilide complex $[Li(OEt_2)][U(=NSiMe_3)(NAdAr)_3]$ (Ar = 3,5-dimethylphenyl),[29] which also exhibited close association of the alkali metal to the nitrogen atom of the imido ligand. The U−N bond length of the imido ligand in **1-K** was 2.010(3) Å, and the average U−N bond length of the amido ligands was 2.378(4) Å, lengthened relative to the corresponding metrics of **1** at 1.910(6) and 2.295(10) Å, respectively,[37] due to the larger ionic radius of the uranium(IV) cation.[76]

In the case of **4-K**, X-ray quality crystals were obtained by crystallization from toluene, following the reaction conducted in THF, filtration over Celite, and removal of the volatiles. In contrast to **1-K**, the K^+ ion is neither coordinated to an aryl solvent nor to the imido ligand but instead interacts with two of the phenyl rings of the trityl group and is solvated by three THF molecules (Figure 4, middle). The U−N bond length of the imido ligand in **4-K** was slightly shorter than in **1-K** at 1.9926(14) Å, and the average U−N bond length of the amido ligands was comparable to those in **1-K** at 2.3870(18)Å. Similar to **1-K**, the U−N bonds in **4-K** are lengthened with respect to its parent uranium(V) complex **4**, which exhibited U−N imido and average amido bond lengths of 1.959(5) and 2.264(3) Å, respectively.

Noting the evidently high charge density at the nitrogen atom of the imido ligands in **1-K** and **6**, as judged by the close association of the K^+ ions in the crystal structures, we investigated the reactivity of these complexes with electrophiles. Additionally, **4-K** was reacted with electrophiles for comparison. To the best of our knowledge, there are no examples of direct addition of an electrophile to a uranium imido complex, though the multiple-bond metathesis reactivity has been noted previously,[39] and similar reactivity was observed by Liddle and co-workers in the silylation of the uranium(V) nitride, $[Na(12\text{-crown-4})_2][U^V(\equiv N)(Tren^{TIPS})]$, $Tren^{TIPS}$ = $N(CH_2CH_2NSi^iPr_3)_3$, to form $U^V(=NSiMe_3)(Tren^{TIPS})$.[5] Silylation of an imido was also implicated in the formation of an unusual uranium(IV) azido amide complex, $[K(18\text{-crown-6})][U(N_3)[N(SiMe_3)_2][OSi(O^tBu)_3]_3]$, obtained from the reaction of $[K(18\text{-crown-6})][U[OSi(O^tBu)_3]_4]$ with Me_3SiN_3, though only as a minor side product.[7] The methylation of **1-K** with MeOTf was carried out successfully, which cleanly produced $U^{IV}[N(SiMe_3)Me][N(SiMe_3)_2]_3$ (**7**) in 68% yield (Scheme 4). In contrast, the addition of Me_3SiOTf to **1-K** led

dx.doi.org/10.1021/ic501149u | Inorg. Chem. 2014, 53, 9129−9139

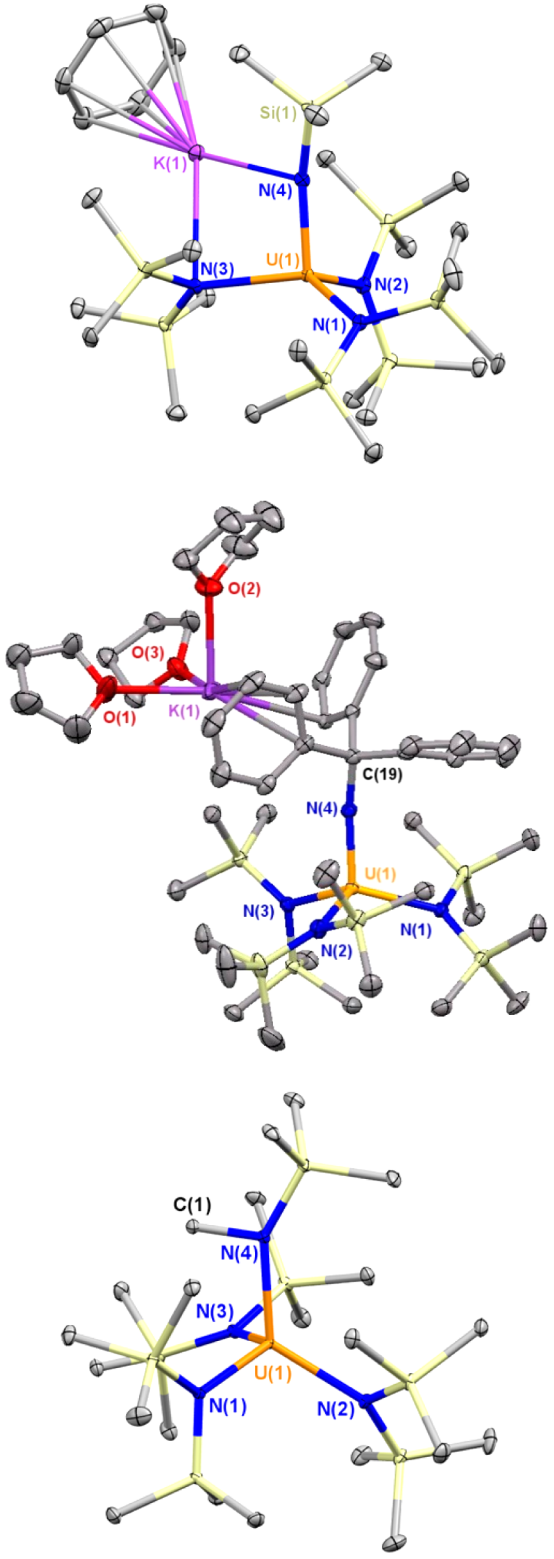

Figure 4. Thermal ellipsoid plot of **1-K** (top), **4-K** (middle), and **7** (bottom) at 30% probability. Hydrogen atoms are omitted for clarity. Bond lengths (Å) and angles (deg), **1-K**: U(1)−N(1) 2.368(3), U(1)−N(2) 2.352(3), U(1)−N(3) 2.415(3), U(1)−N(4) 2.010(3), U(1)−N(4)−Si(1) 156.90(16). **4-K**: U(1)−N(1) 2.3870(14), U(1)−N(2) 2.3763(15), U(1)−N(3) 2.3978(14), U(1)−N(4) 1.9926(14), U(1)−N(4)−C(19) 169.82(12). **7**: U(1)−N(1) 2.290(2), U(1)−N(2) 2.2978(19), U(1)−N(3) 2.2786(17), U(1)−N(4) 2.2168(19), U(1)−N(4)−C(1) 99.79(13).

to formation of a complex mixture of products that did not include the known complex $U^{IV}[N(SiMe_3)_2]_4$.[74]

The ^{1}H NMR of **7** displayed a single, broad resonance for the three bis(trimethylsilyl)amide ligands at −4.6 ppm and two sharp resonances for the methyl(trimethylsilyl)amide ligand at 76.9 and −3.3 ppm, indicating that the trimethylsilyl groups freely rotated at room temperature. The X-ray structure of **7** (Figure 4, bottom) exhibited close contact of the added methyl group with the uranium center, with a U−C distance of 2.869 Å. The close contact of the methyl group with the uranium ion is nearly in the range of some uranium−carbon single bonds.[77,78] This structural perturbation is also evident in the acute U−N−C bond angle, at 99.79°. The U−N bond lengths of the $-N(SiMe_3)_2$ ligands were on average 2.289 Å, similar to those of $U[N(SiMe_3)_2]_4$ at 2.297(2) Å.[74] Reaction of **4-K** with Me_3SiOTf or MeI resulted in oxidation of **4-K** to yield **4** and unidentified side products (Scheme 4). This reactivity differed from that of **1-K** possibly due to the decrease in charge density at the imido nitrogen atom in **4-K**, as evidenced by the coordination of the K^+ ion with the trityl aryl groups instead of the imido nitrogen atom in its solid state structure. Reaction of **4-K** with MeOTf resulted in a mixture of as yet unidentified products.

The reactivity of **6** with electrophiles was also not straightforward. We attempted to silylate the imido to form the homoleptic tetrakis(amide) $U^{IV}[N(SiMe_3)Ph^F]_4$ (**8**). As a basis for comparison, the synthesis of **8** was carried out directly from the reaction of $UI_4(OEt_2)_2$ with 4 equiv of $KN(SiMe_3)$-Ph^F. The addition of Me_3SiI to **6** produced **8** as a minor product, with significant amounts of as yet uncharacterized side products, limiting the utility of this reaction. Use of the more potent electrophile Me_3SiOTf resulted in decomposition to a mixture of unidentified products.

Electrochemistry. Electrochemical analysis yielded insight into the different imido complexes (Table 2). In the previous report of the cyclic voltammetry of **1**, a reversible oxidation feature at −0.41 V versus ferrocene was observed in THF, with $[^nBu_4N][BF_4]$ serving as the electrolyte.[30] The cyclic voltammograms of **1** and **4** were collected in dichloromethane with $[^nBu_4N][PF_6]$ electrolyte (Figure 5). An irreversible

Table 2. Reduction Potentials of the Imido Complexes Determined by DPV Measurements, Compared to the Previously Reported Mono-Oxo Complexes[32,33]

	$E_{1/2}$ (V)	
	U(VI/V)	U(V/IV)
1 $U^V(=NSiMe_3)(N^*)_3$[a]	+0.26	−1.35
4 $U^V(=NCPh_3)(N^*)_3$[a]	+0.38	−1.31
2-Br $U^{VI}(=NSiMe_3)Br(N^*)_3$[a]	−0.40	−1.28
2-Cl $U^{VI}(=NSiMe_3)Cl(N^*)_3$[a]	−0.47	−1.25
2-O $[Ph_4P][U^{VI}(=NSiMe_3)O(N^*)_3]$[a]	−2.34	
3-Br[32,33] $U^{VI}OBr(N^*)_3$[a]	−0.21	
3-Cl[32,33] $U^{VI}OCl(N^*)_3$[a]	−0.43	

[a]$N^* = N(SiMe_3)_2$.

dx.doi.org/10.1021/ic501149u | Inorg. Chem. 2014, 53, 9129−9139

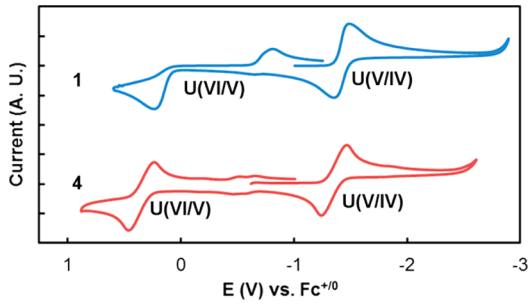

Figure 5. Cyclic voltammogram of **1** (top) and **4** (bottom) in CH_2Cl_2, at a scan rate of 250 mV/s with 0.1 M $[^nBu_4N][PF_6]$ electrolyte.

U(VI/V) couple was observed in **1**, with an E_{pa} of +0.21 V and an E_{pc} of −0.79 V. The $E_{1/2}$ of this couple was obtained from the differential pulse voltammogram, which revealed a reversible potential of +0.26 V. Therefore, the apparent irreversibility of this couple is attributed to a large overpotential in the cathodic wave. By comparison, the U(VI/V) couple in **4** was reversible under all conditions, at a potential of +0.38 V. The higher potential U(VI/V) couple in **4** relative to **1** indicates that the trimethylsilylimido ligand more significantly stabilizes the +6 oxidation state than the electron deficient tritylimido ligand. The U(V/IV) couple was reversible in both complexes, appearing at −1.35 V in **1** and −1.31 V in **4**.

The strong donating ability of the trimethylsilylimido ligand in **1** led us to consider its ability to stabilize the U(VI) oxidation state relative to the oxo ligand. Cyclic voltammetry was collected on **2-Br** and **2-Cl** for comparison to the corresponding oxo-halides.[77,78] The cyclic voltammogram of **2-Br** displayed two redox features (Figure 6), assigned as a

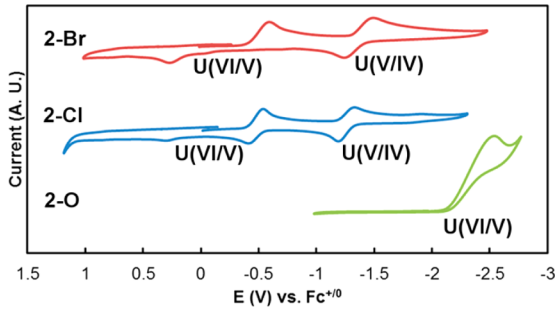

Figure 6. Cyclic voltammetry of **2-Br** (top), **2-Cl** (middle), and **2-O** (bottom) at a scan rate of 250 mV/s in CH_2Cl_2, with 0.1 M $[^nBu_4N][PF_6]$ supporting electrolyte.

quasi-reversible U(VI/V) couple centered at −0.40 V and a reversible U(V/IV) couple at −1.28 V.[79] The poor reversibility of the first reduction feature is due to a large overpotential in the return oxidation wave, with low current intensity. This behavior is attributed to chemical loss of the bromide ligand upon reduction. In contrast, the two redox couples were reversible in **2-Cl**, centered at −0.47 and −1.25 V, respectively. Surprisingly, in both **2-Br** and **2-Cl**, the U(VI/V) couples were at more reducing potentials than the analogous features in **3-Br** and **3-Cl**, which appear at −0.21 and −0.43 V, respectively, indicating that the stabilization of the +6 oxidation state is comparable in the presence of either the trimethylsilylimido ligand or the oxo ligand. The cyclic voltammogram of **2-O** revealed a significant shift in the U(VI/V) couple, exhibiting an irreversible reduction identified from differential pulse voltammetry (DPV) at −2.34 V (Figure S9). The strong stabilization of the +6 oxidation state in **2-O** is reminiscent of complexes of $U^{VI}O_2^{2+}$.[80]

Electronic Structure Calculations. A comparison of the ground-state electronic structure of **1** and **4** was carried out to assess their relative stabilities. The calculated natural charge on the uranium ion on each of the complexes was approximately equal, at +1.99 and +2.00. However, the natural charge on the nitrogen atom of the imido ligand was −1.23 in **1** and −0.81 in **4**. These values suggest that while the overall charge donation to the uranium ion is the same, the polarization of the U═N bond, which is a favorable effect for stabilizing high valent uranium complexes, is greater in **1** than in **4** (*vide infra*).

In previous work by Andersen and co-workers, comparison of the compounds $Cp_2U^{IV}O$ and Cp_2U^{IV}(═NMe) led to the conclusion that although the uranium−oxo bond was less covalent than the uranium−imido bond, the highly polarized U−O bond was stronger.[81] Following a similar analysis, NBO 6.0[82] calculation of the U−N σ-bonding interaction in **2-Cl** showed a bond comprising a 21.9% contribution from uranium, consisting of 39.6% 6d and 56.7% 5f AO character, and a 78.1% contribution from nitrogen. The U−O σ-bonding interaction in **3-Cl** was remarkably similar: a 21.5% uranium contribution originating from 32.3% 6d and 65.5% 5f AO character and 78.5% oxygen AO character. These values suggested similarly ionic bonding in the U═$NSiMe_3$ and U═O fragments. However, the natural charge on the uranium ion was +1.42 in **2-Cl** and +1.62 in **3-Cl**, and the natural charge on the nitrogen atom of the imido ligand was −1.01 in **2-Cl** while the natural charge on the oxo ligand was −0.62 in **3-Cl**. The total natural charge distributed across the entire trimethylsilylimido ligand in **2-Cl** was only −0.43. The smaller charge to formal oxidation state ratio on the uranium center in the imido complex **2-Cl** relative to the oxo complex **3-Cl** represented more covalent bonding,[81] whereas the larger negative charge on the nitrogen atom of the imido ligand compared to the oxo ligand represented greater polarization. Therefore, the trimethylsilylimido ligand preserves the overall enhanced covalency of the imido ligand at the high valent uranium(VI) cation and lends additional stability through favorable polarization.

In order to further probe the ability for the trimethylsilylimido ligand to stabilize the trans-axial geometry, a systematic computational study was carried out to compare the relative energies of cis and trans isomers between theoretical dioxo, oxo/imido, and bis(imido) species. A similar approach has been used to determine the cis/trans isomerization energy of uranyl in $[UO_2(OH)_4]^{2-}$ of 18−19 kcal mol^{-1},[83] as well as that of bis(imido) species including $U(NMe)_2I_2(THF)_2$ at 14.7−16.5 kcal mol^{-1} [12] and $U(NPh)_2I_2(THF)_n$ (n = 2, 3) at 7.6−14.8 kcal mol^{-1}.[34] However, to the best of our knowledge, no previous analysis has compared the effect of oxo/imido substitution or the impact of imido functionality on cis/trans isomerization energy.

Truncated model complexes of the formulas *cis*/*trans*-$[U^{VI}O_n(NR)_{2-n}[N(SiH_3)_2]_3]^-$ were investigated (Figure 7), where methyl groups of the equatorial amide ligands were removed to minimize steric effects. As a benchmark for comparison, the *trans*-UO_2 geometry was calculated to be 31.4 kcal mol^{-1} more stable than the *cis*-UO_2 configuration. Upon substitution of one oxo ligand with a trimethlylsilylimido ligand, the *trans*-UO(═$NSiMe_3$) structure was only 18.0 kcal mol^{-1} more stable than the most stable *cis*-UO(═$NSiMe_3$) isomer. Further substitution to the bis(imido) complex showed a

dx.doi.org/10.1021/ic501149u | Inorg. Chem. 2014, 53, 9129−9139

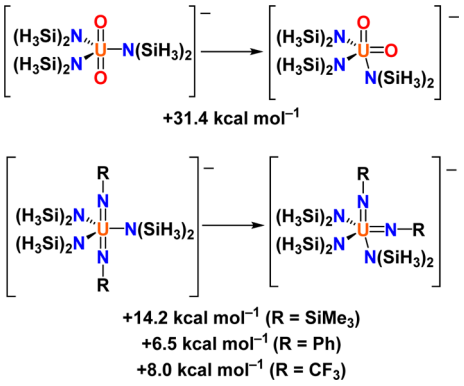

Figure 7. DFT calculated cis/trans isomerization free energies of related uranyl and uranium bis(imido) complexes.

further reduction of the cis/trans isomerization free energy to 14.2 kcal mol^{-1}. Therefore, while the trans-stabilization of the trimethylsilylimido ligand is slightly larger than that of the oxo ligand on the basis of structural analysis and consideration of electrochemical potential, the *cis*-UO_2 configuration is more destabilized. The natural charges on the imido nitrogen atoms ranged from −0.62 in the case of the phenyl imido derivative to −1.06 and −1.10 in the case of the more donating trimethylsilyl derivative. The natural charges on the oxo groups were comparable with the phenyl imido derivative with charges −0.62 and −0.67 (Figure S15).

Finally, comparison of two additional imido derivatives was pursued to confirm the stabilization provided by the trimethylsilyl group. Determination of the isomerization free energies of $[U^{VI}(NR)_2[N(SiH_3)_2]_3]^-$ (R = $-SiMe_3$, −Ph, $-CF_3$) showed the strongest stabilization of the trans geometry in the trimethylsilyl derivative, at 14.2 kcal mol^{-1}, 6.5 kcal mol^{-1}, and 8.0 kcal mol^{-1}, respectively. Expanding this analysis to the $[U^{VI}O(NR)[N(SiH_3)_2]_3]^-$ complexes provided the same trend, at 18.0 kcal mol^{-1}, 13.5 kcal mol^{-1}, and 15.1 kcal mol^{-1}.

Analysis of Thermodynamics of Uranium Imido Formation. The divergent reactivity exhibited by the monoimido complexes **1** and **4** led us to consider the thermodynamics of these processes (Figure 8). Since Me_3SiN_3 and Ph_3CN_3 may act as either one-electron or two-electron oxidants, but the uranium(IV) azide intermediate was only observed in the synthesis of **4**; the relative free energy changes of these processes were compared. The formation of the monoimido complexes **1** and **4** were found to be exothermic in both cases, with calculated ΔG_{rxn} = −41.9 and −30.5 kcal mol^{-1}, respectively, reflecting the greater stabilization of the trimethylsilylimido ligand relative to the tritylimido ligand.

The formation of the intermediate uranium(IV) azide complex through Si−N bond homolysis was endothermic by +18.1 kcal mol^{-1}, whereas the C−N bond homolysis route for trityl azide was exothermic by −35.3 kcal mol^{-1}. Reversibility of the C−N bond homolysis was unfavorable, as the uranium(III) tritylazide adduct was predicted to be unstable relative to the uranium(IV) azide by 33.8 kcal mol^{-1}. The ability to isolate this product at low temperature suggests that the direct one-electron oxidation to form **4** possesses a large kinetic barrier. This observation indicates that *N*-methylmorpholine-*N*-oxide facilitates the one-electron transfer process, most likely through transient coordination to the uranium ion. As an alternative mechanism, the two-electron reduction of azide may be

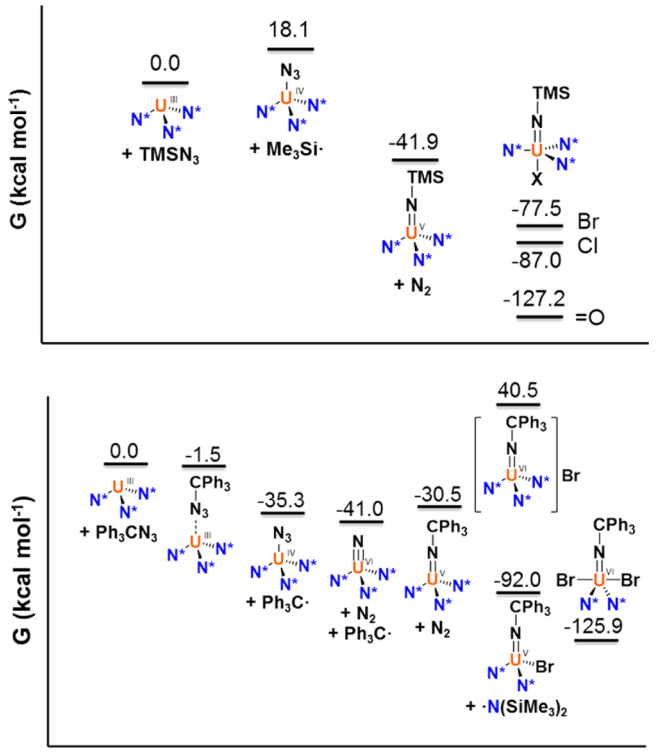

Figure 8. DFT computed thermodynamics of the oxidation reactions involved in the synthesis of the uranium monoimido complexes.

facilitated to generate the uranium(VI) nitrido complex which may recombine with the trityl radical to form **4**. Similar reactivity has been observed in the reaction of the iron(IV) nitrido complex, $[PhB(MesIm)_3Fe^{IV}{\equiv}N]$,[84] with the trityl radical to form the iron(III) imido complex, $[PhB(MesIm)_3Fe^{IV}{=}NCPh_3]$,[85] though the only reactivity of uranium(VI) nitrido complexes that has been reported thus far has been C−H activation.[4,86] Calculation of the hypothetical uranium(VI) nitrido intermediate showed that it was in fact more energetically favorable than **4**, suggesting that it may exist as an intermediate in this reaction.

Oxidation of **1** to form **2-Br**, **2-Cl**, and **2-O** was found to be exothermic. In contrast, the product of oxidation of **4** contained an outer sphere bromide ion due to the steric hindrance of the trityl group. Although this product was predicted to be highly unstable, the products of sterically induced reduction, $U^{V}Br(=NSiMe_3)[N(SiMe_3)_2]_2$ and $^{\bullet}N(SiMe_3)_2$, were predicted to be much lower in energy, consistent with the experimental observation. Further oxidation of this coordinatively unsaturated uranium(V) intermediate to form **5** was also determined to be favorable. These results suggest that the formation of **5** proceeds through sterically induced reduction followed by oxidation of the metal ion rather than through an outer sphere oxidation pathway.

CONCLUSIONS

The reactivity and increase in donating ability, with respect to analogous uranium(VI) oxo complexes, of the uranium imido complexes shown here demonstrates that there is still much to learn about the behavior of complexes bearing uranium−nitrogen multiple bonds. In this work, we observed the unexpected one-electron transfer reactions involved in the preparation of uranium monoimido complexes in the +4, +5, and +6 oxidation states. Among these was the stepwise

dx.doi.org/10.1021/ic501149u | Inorg. Chem. 2014, 53, 9129−9139

formation of a uranium(V) tritylimido complex, the first direct synthesis of a uranium oxo/imido complex through one-electron oxidation, an unusual sterically induced reduction reaction induced by the bulky trityl group to form a uranium(VI) dibromide, and the direct synthesis of a uranium(IV) imido through the loss of a trimethylsilyl group. The uranium(IV)−imido complexes were additionally found to be reactive toward electrophiles. Future work will focus on expanding the one-electron reactivity of uranium monoimido complexes and investigating the ITI strength of substituted imido derivatives toward stabilizing reactive uranium-ligand bonds.

EXPERIMENTAL SECTION

General Methods. All reactions and manipulations were performed under an inert atmosphere (N_2) using standard Schlenk techniques or in a Vacuum Atmospheres, Inc. Nexus II drybox equipped with a molecular sieves 13X/Q5 Cu-0226S catalyst purifier system. Glassware was oven-dried overnight at 150 °C prior to use. ^{1}H NMR were obtained on a Bruker DMX-300 Fourier transform NMR spectrometer at 300 MHz. Chemical shifts were recorded in units of parts per million downfield from residual proteo solvent peaks. Elemental analyses were performed at the University of California, Berkeley Microanalytical Facility using a PerkinElmer Series II 2400 CHNS analyzer or at Complete Analysis Laboratories, Inc. using a Carlo Erba EA 1108 analyzer. The infrared spectra were obtained from 400 to 4000 cm^{-1} using a PerkinElmer 1600 series infrared spectrometer.

Materials. Tetrahydrofuran, Et_2O, CH_2Cl_2, hexanes, pentane, and toluene were purchased from Fisher Scientific. These solvents were sparged for 20 min with dry argon and dried using a commercial two-column solvent purification system comprising columns packed with Q5 reactant and neutral alumina, respectively (for hexanes and pentane), or two columns of neutral alumina (for THF, Et_2O, and CH_2Cl_2). All solvents were stored over 3 Å molecular sieves. Deuterated solvents were purchased from Cambridge Isotope Laboratories, Inc. and stored over a potassium mirror overnight prior to use. Starting materials, $UI_3(THF)_4$,[87] $UI_4(OEt_2)_2$,[88] $U[N(SiMe_3)_2]_3$,[89] **1**,[37] and $K[N(SiMe_3)Ph^F]$,[90] were prepared according to the reported procedures.

Electrochemistry. Voltammetry experiments (CV, DPV) were performed using a CH Instruments 620D Electrochemical Analyzer/Workstation, and the data were processed using CHI software v9.24. All experiments were performed in a N_2 atmosphere drybox using electrochemical cells that consisted of a 4 mL vial, glassy carbon working electrode, a platinum wire counter electrode, and a silver wire plated with AgCl as a quasi-reference electrode. The quasi-reference electrode was prepared by dipping a length of silver wire in concentrated hydrochloric acid. The working electrode surfaces were polished prior to each set of experiments. Potentials were reported versus ferrocene, which was added as an internal standard for calibration at the end of each run. Solutions employed during these studies were ∼3 mM in analyte and 100 mM in $[^nBu_4N][PF_6]$ in 2 mL of dichloromethane. All data were collected in a positive-feedback IR compensation mode.

X-Ray Crystallography. X-ray intensity data were collected on a Bruker APEXII CCD area detector employing graphite-monochromated Mo Kα radiation (λ = 0.71073 Å) at a temperature of 143(1) K. In all cases, rotation frames were integrated using SAINT,[91] producing a listing of unaveraged F^2 and $\sigma(F^2)$ values which were then passed to the SHELXTL[92] program package for further processing and structure solution. The intensity data were corrected for Lorentz and polarization effects and for absorption using TWINABS[93] or SADABS.[94] The structures were solved by direct methods (SHELXS-97).[95] Refinement was by full-matrix least-squares based on F^2 using SHELXL-97.[95] All reflections were used during refinements. Non-hydrogen atoms were refined anisotropically and hydrogen atoms were refined using a riding model.

Computational Details. All calculations were performed with Gaussian 09, revision D.01,[96] with the B3LYP hybrid DFT method. An effective core potential incorporating quasi-relativistic effects was applied to uranium, with a 60 electron core and the corresponding segmented natural orbital basis set.[97,98] The 6-31G* basis set was used for all small molecules.[99] Geometry optimizations were carried out in C_1 symmetry for all uranium complexes and all small molecules, as higher symmetry solutions were either higher in energy or were not successfully converged. Default settings were used for the integration grid, SCF, and geometry convergence criteria. All frequency calculations found no imaginary frequencies, confirming that the optimized structures were minima.

Synthesis of $U(=NSiMe_3)Br[N(SiMe_3)_2]_3$ (2-Br). To a stirred solution of $U[(NSiMe_3)_2]_3$ (150 mg, 0.20 mmol, 1.00 equiv) in hexanes was added trimethylsilyl azide (23 mg, 0.20 mmol, 1.00 equiv). After stirring for 10 min, the volatiles were removed under reduced pressure. The crude reaction mixture was dissolved in THF, and $CuBr_2$ (228 mg, 1.02 mmol, 5.00 equiv) was added. After stirring for 1 h, the reaction mixture was filtered over Celite suspended in a glass pipet, and the volatiles were removed under reduced pressure. The resulting residue was extracted with hexanes, filtered over Celite, and recrystallized from minimal hexanes to yield **2-Br** as a dark red solid. Yield: 130 mg, 0.15 mmol, 79%. ^{1}H NMR (benzene-d_6): 0.84 (27H), 0.71 (27 H), −0.05 (9H). IR (Nujol mull): 1302 (vw), 1249 (s), 1170 (vw), 1109 (vw), 982 (vw), 922 (m), 848 (vs), 773 (m), 722 (vw), 654 (s), 621 (m), 566 (vw) cm^{-1}. Elemental analysis found (calculated) for $C_{21}H_{63}BrN_4Si_7U$: C, 28.32 (28.46); H 6.96 (7.17); N 6.16 (6.32).

Synthesis of $U(=NSiMe_3)Cl[N(SiMe_3)_2]_3$ (2-Cl). To a stirred solution of $U[(NSiMe_3)_2]_3$ (150 mg, 0.20 mmol, 1.00 equiv) in hexanes was added trimethylsilyl azide (23 mg, 0.20 mmol, 1.00 equiv). After stirring for 10 min, the volatiles were removed under reduced pressure. The crude reaction mixture was dissolved in THF, and $CuCl_2$ (137 mg, 1.02 mmol, 5.00 equiv) was added. After stirring for 1 h, the reaction mixture was filtered over Celite suspended in a glass pipet, and the volatiles were removed under reduced pressure. The resulting residue was extracted with hexanes, filtered over Celite, and recrystallized from minimal hexanes to yield **2-Cl** as a dark red solid. Yield: 70 mg, 0.08 mmol, 45%. ^{1}H NMR (benzene-d_6): 0.84 (27H), 0.62 (27 H), 0.00 (9H). IR (Nujol mull): 1303 (vw), 1261 (m), 1248 (s), 1152 (vw), 1085 (vw), 922 (m), 848 (vs), 774 (m), 722 (w), 698 (vw), 681 (vw), 654 (s), 621 (m). Elemental analysis found (calculated) for $C_{21}H_{63}ClN_4Si_7U$: C, 29.89 (29.96); H 7.59 (7.54); N 6.48 (6.66).

Synthesis of $Ph_4P[U(=NSiMe_3)O[N(SiMe_3)_2]_3]$ (2-O). To a stirred solution of $U[(NSiMe_3)_2]_3$ (100 mg, 0.14 mmol, 1.00 equiv) in hexanes was added trimethylsilyl azide (16 mg, 0.14 mmol, 1.00 equiv). The crude reaction mixture was dissolved in THF, and tetraphenylphosphonium nitrite (61 mg, 0.16 mmol, 1.1 equiv) was added. After stirring for 10 min, the mixture was filtered over Celite suspended in a glass pipet, and the volatiles were removed under reduced pressure. The product was then dissolved in toluene and layered with pentane to yield **2-O** as a dark orange solid. Yield: 99 mg, 0.09 mmol, 69%. ^{1}H NMR (benzene-d_6): 8.19 (8 H), 8.09 (4 H), 7.83 (8 H), 0.91 (54 H), 0.09 (9 H). IR (Nujol mull): 2187 (w), 2081 (w), 1241 (m), 1109 (m), 1026 (w), 999 (w), 951 (s), 838 (s), 774 (w), 754 (w), 723 (m), 689 (m), 662 (m), 607 (w), 526 (m). Elemental analysis found (calculated) for $C_{45}H_{83}N_4OPSi_7U$: C, 46.36 (46.52); H 7.09 (7.20); N 4.69 (4.82).

Synthesis of $U(=NCPh_3)[N(SiMe_3)_2]_3$ (4). To a solution of $U[N(SiMe_3)_2]_3$ (200 mg, 0.28 mmol) in 10 mL Et_2O cooled to −21 °C, Ph_3CN_3 (80 mg, 0.28 mmol, 1.00 equiv) was added, resulting in an immediate color change to pale brown. After stirring for 15 min, *N*-methylmorpholine-*N*-oxide (66 mg, 0.56 mmol, 2.00 equiv) was added, resulting in the immediate evolution of gas and a color change to dark green. The mixture was stirred for 20 min, and after filtration through Celite suspended in a glass pipet, the volatiles were removed under reduced pressure. Recrystallization from minimal hexanes at −21 °C afforded **4** as a green-black crystalline solid. Yield: 272 mg, 0.28 mmol, 93%. ^{1}H NMR (benzene-d_6): 22.31 (6H), 10.20 (6H),

dx.doi.org/10.1021/ic501149u | Inorg. Chem. 2014, 53, 9129−9139

8.71 (3H), −3.94 (54H). Elemental analysis found (calculated) for $C_{37}H_{69}N_4Si_6U$: C, 45.58 (45.51); H 7.02 (7.12); N 5.75 (5.74).

Synthesis of U(=NCPh$_3$)Br$_2$[N(SiMe$_3$)$_2$]$_2$ (5). To a solution of **4** (40 mg, 0.04 mmol) in 5 mL of THF, $CuBr_2$ (46 mg, 0.21 mmol, 5.00 equiv) was added. After stirring for 10 min, the volatiles were removed under reduced pressure. The resulting residue was extracted with pentane, filtered through Celite suspended in a glass pipet, and stored at −21 °C to yield dark red-brown needles of **5**. Yield: 33 mg, 0.03 mmol, 83%. ^{1}H NMR (benzene-d_6): 7.72 (3H), 7.35 (6H), 7.02 (6H), 0.72 (36H). Elemental analysis found (calculated) for $C_{31}H_{51}Br_2N_3Si_4U$: C, 37.91 (38.15); H, 4.94 (5.27); N, 4.20 (4.31).

Synthesis of K[U(=NCPh$_3$)[N(SiMe$_3$)$_2$]$_3$] (4-K). To a solution of **4** (58 mg, 0.06 mmol) in 4 mL of THF, KC_8 (8 mg, 0.06 mmol, 1.00 equiv) was added. After stirring for 10 min, the reaction mixture was filtered over Celite, and the volatiles were removed under reduced pressure. The crude material was recrystallized from minimal toluene at −21 °C to yield pale orange crystals of **4-K**. Yield: 30 mg, 0.03 mmol, 50%. ^{1}H NMR (benzene-d_6): 41.10 (6H), 13.79 (6H), 11.98 (3H), −8.92 (54 H). Compound **4-K** was chemically unstable toward evacuation; it decomposed to an insoluble, as yet uncharacterized gray solid upon exposure to a vacuum. Elemental analysis was attempted for **4-K** but was unobtainable due to its instability.

Synthesis of K(THF)U^{IV}(=NPh^F)(NTMSPh^F)$_3$ (6). To a vial containing $UI_3(thf)_4$ (91 mg, 0.1 mmol, 1.00 equiv) dissolved in 2 mL of thf, a 2 mL thf solution of KNTMSPh^F (88 mg, 0.3 mmol, 3.00 equiv) was added, resulting in a color change to red and precipitation. The mixture was stirred for 0.5 h and filtered through Celite suspended in a glass pipet. The volatiles were removed under reduced pressure. The residue was extracted with hexanes and filtered through Celite suspended in a glass pipet. The hexanes solution was concentrated to 0.5 mL and stored at −21 °C to yield orange crystals of **6**. Yield: 17 mg, 0.013 mmol, 17%. ^{1}H NMR (thf): δ 0.22 (s, 27H, −SiMe$_3$).^{19}F NMR (thf): δ −114.28 (s, 2F, *o*-F imido), −146.32 (t, 2F, *m*-F imido, J = 23 Hz), −167.98 (d, 6F, *m*-F amide, J = 20 Hz), −171.75 (t, 3F, *p*-F amide, J = 23 Hz), −174.47 (t, 1F, *p*-F imido, J = 23 Hz), −187.21 (br, 6F, *o*-F amide, fwhm =130 Hz). Elemental analysis found (calculated) for $C_{37}H_{35}F_{20}KN_4OSi_3U$: C, 34.49 (34.37); H 3.15 (2.73); N 3.89 (4.33).

Synthesis of K[U(=NSiMe$_3$)[N(SiMe$_3$)$_2$]$_3$] (1-K). To a stirred solution of U[(NSiMe$_3$)$_2$]$_3$ (100 mg, 0.14 mmol, 1.00 equiv) in hexanes was added trimethylsilyl azide (16 mg, 0.14 mmol, 1.00 equiv). The crude reaction mixture was dissolved in THF and cooled to −21 °C before adding KC_8 (28 mg, 0.20 mmol, 1.5 equiv) and stirring for 10 min. The mixture was then filtered over Celite suspended in a glass pipet, and the volatiles were removed under reduced pressure. The resulting residue was extracted with pentane and filtered over Celite, and the volatiles were removed under reduced pressure. The residue was dissolved in benzene, and the volatiles were removed under reduced pressure before crystallizing the product from a small volume of pentane to yield **1-K** as a light pink solid. X-ray structural analysis of a sample prepared with benzene-d_6 indicated that **1-K** crystallized as [K(C$_6$D$_6$)][U(=NSiMe$_3$)[N(SiMe$_3$)$_2$]$_3$, though desolvation was confirmed by elemental analysis. Yield: 112 mg, 0.12 mmol, 87%. ^{1}H NMR (benzene-d_6): 34.63 (9H), −7.87 (54 H). IR (Nujol mull): 2205 (w), 2101 (w), 1249 (s), 1180 (w), 1012 (s), 944 (s), 840 (s), 770 (m), 663 (m), 601 (m), 511 (w). Elemental analysis found (calculated) for $C_{21}H_{63}KN_4Si_7U$: C, 29.52 (29.83); H 7.49 (7.51); N 6.32 (6.63).

Synthesis of U[NMe(SiMe$_3$)][N(SiMe$_3$)$_2$]$_3$ (7). To a stirred solution of **1-K** (239 mg, 0.26 mmol, 1 equiv) in hexanes was added methyl triflate (63 mg, 0.386 mmol, 1.5 equiv). The reaction mixture was stirred for 10 min and filtered over Celite suspended in a glass pipet, and the volatiles were removed under reduced pressure. Recrystallization from minimal (SiMe$_3$)$_2$O at −21 °C gave light brown crystals of **7**. Yield: 144 mg, 0.18 mmol, 68%. ^{1}H NMR (benzene-d_6): 76.93 (3 H), −3.21 (9 H), −4.63 (54 H). IR (Nujol mull): 1250 (m), 904 (s), 848 (s), 772 (m), 722 (m), 666 (w), 612 (w). Elemental analysis found (calculated) for $C_{22}H_{66}N_4Si_7U$: C, 31.78 (32.17); H, 7.99 (8.10); N, 6.54 (6.82).

Synthesis of U[N(SiMe$_3$)Ph^F]$_4$ (8). To a vial containing $UI_4(Et_2O)_2$ (89 mg, 0.1 mmol, 1.00 equiv) dissolved in 3 mL Et_2O, an Et_2O solution containing KN(SiMe$_3$)Ph^F (117 mg, 0.4 mmol, 4.00 equiv) was slowly added, causing an immediate color change to red and precipitation. After stirring for 1 h, the slurry was filtered through Celite suspended in a glass pipet and washed with 2 × 2 mL Et_2O. The volatiles were removed under reduced pressure. Hexanes (5 mL) was added, and the mixture was heated to boiling and then filtered through Celite suspended in a glass pipet to yield an orange filtrate. The hexanes solution was concentrated to about 0.5 mL and stored at −21 °C to yield orange crystals of **8** which were collected and dried under reduced pressure. Yield: 31 mg, 0.025 mmol, 25%. ^{1}H NMR (C$_6$D$_6$): δ −10.23 (s, 36H, −SiMe$_3$).^{19}F NMR (C$_6$D$_6$): δ −144.58 (br, 8F, *o*-F, fwhm = 73 Hz), −156.80 (t, 4F, *p*-F, J = 23 Hz), −164.87 (t, 8F, *m*-F, J = 23 Hz). Elemental analysis found (calculated) for $C_{36}H_{36}F_{20}N_4Si_4U$: C, 34.13 (34.45); H, 2.74 (2.89); N, 4.34 (4.46).

■ ASSOCIATED CONTENT

Supporting Information

Crystallographic data (CIFs), electrochemical data, UV−vis−NIR data, and computational details. This material is available free of charge via the Internet at http://pubs.acs.org.

■ AUTHOR INFORMATION

Corresponding Author

*E-mail: schelter@sas.upenn.edu.

Notes

The authors declare no competing financial interest.

■ ACKNOWLEDGMENTS

We gratefully acknowledge the National Science Foundation (CHE-1362854), Research Corporation for Science Advancement (Cottrell Scholar Award to E.J.S.) and the University of Pennsylvania for financial support. We also thank the U.S. National Science Foundation for support of the X-ray diffractometer used in this work (CHE-0840438). This work used the Extreme Science and Engineering Discovery Environment (XSEDE), which is supported by U.S. National Science Foundation grant number OCI-1053575. We thank Prof. Christopher R. Graves (Albright College) for helpful discussion. We are also grateful to Prof. Donald H. Berry (University of Pennsylvania) for assistance in running NBO 6.0 calculations in the revision of this manuscript.

■ REFERENCES

(1) Hayton, T. W. *Chem. Commun.* **2013**, *49*, 2956−2973.
(2) Hayton, T. W. *Dalton Trans.* **2010**, *39*, 1145−1158.
(3) King, D. M.; McMaster, J.; Tuna, F.; McInnes, E. J. L.; Lewis, W.; Blake, A. J.; Liddle, S. T. *J. Am. Chem. Soc.* **2014**, *136*, 5619−5622.
(4) King, D. M.; Tuna, F.; McInnes, E. J. L.; McMaster, J.; Lewis, W.; Blake, A. J.; Liddle, S. T. *Nat. Chem.* **2013**, *5*, 482−488.
(5) King, D. M.; Tuna, F.; McInnes, E. J. L.; McMaster, J.; Lewis, W.; Blake, A. J.; Liddle, S. T. *Science* **2012**, *337*, 717−720.
(6) King, D. M.; Liddle, S. T. *Coord. Chem. Rev.* **2014**, *266−267*, 2−15.
(7) Camp, C.; Pécaut, J.; Mazzanti, M. *J. Am. Chem. Soc.* **2013**, *135*, 12101−12111.
(8) Arney, D. S. J.; Burns, C. J.; Smith, D. C. *J. Am. Chem. Soc.* **1992**, *114*, 10068−10069.
(9) Warner, B. P.; Scott, B. L.; Burns, C. J. *Angew. Chem., Int. Ed.* **1998**, *37*, 959−960.
(10) Kiplinger, J. L.; Morris, D. E.; Scott, B. L.; Burns, C. J. *Chem. Commun.* **2002**, *2002*, 30.
(11) Hayton, T. W.; Boncella, J. M.; Scott, B. L.; Palmer, P. D.; Batista, E. R.; Hay, P. J. *Science* **2005**, *310*, 1941−1943.

(12) Hayton, T. W.; Boncella, J. M.; Scott, B. L.; Batista, E. R.; Hay, P. J. *J. Am. Chem. Soc.* **2006**, *128*, 10549−10559.
(13) Hayton, T. W.; Boncella, J. M.; Scott, B. L.; Batista, E. R. *J. Am. Chem. Soc.* **2006**, *128*, 12622−12623.
(14) Spencer, L. P.; Yang, P.; Scott, B. L.; Batista, E. R.; Boncella, J. M. *J. Am. Chem. Soc.* **2008**, *130*, 2930−2931.
(15) Spencer, L. P.; Gdula, R. L.; Hayton, T. W.; Scott, B. L.; Boncella, J. M. *Chem. Commun.* **2008**, *2008*, 4986−4988.
(16) Spencer, L. P.; Schelter, E. J.; Yang, P.; Gdula, R. L.; Scott, B. L.; Thompson, J. D.; Kiplinger, J. L.; Batista, E. R.; Boncella, J. M. *Angew. Chem., Int. Ed.* **2009**, *48*, 3795−3798.
(17) Evans, W. J.; Traina, C. A.; Ziller, J. W. *J. Am. Chem. Soc.* **2009**, *131*, 17473−17481.
(18) Spencer, L. P.; Yang, P.; Scott, B. L.; Batista, E. R.; Boncella, J. M. *Inorg. Chem.* **2009**, *48*, 2693−2700.
(19) Spencer, L. P.; Yang, P.; Scott, B. L.; Batista, E. R.; Boncella, J. M. *C. R. Chim.* **2010**, *13*, 758−766.
(20) D, L. S., II; Spencer, L. P.; Scott, B. L.; Odom, A. L.; Boncella, J. M. *Dalton Trans.* **2010**, *39*, 6841−6846.
(21) Seaman, L. A.; Fortier, S.; Wu, G.; Hayton, T. W. *Inorg. Chem.* **2011**, *50*, 636−646.
(22) Jilek, R. E.; Spencer, L. P.; Lewis, R. A.; Scott, B. L.; Hayton, T. W.; Boncella, J. M. *J. Am. Chem. Soc.* **2012**, *134*, 9876−9878.
(23) Cladis, D. P.; Kiernicki, J. J.; Fanwick, P. E.; Bart, S. C. *Chem. Commun.* **2013**, *49*, 4169−4171.
(24) Arney, D. S. J.; Burns, C. J. *J. Am. Chem. Soc.* **1993**, *115*, 9840−9841.
(25) Jilek, R. E.; Spencer, L. P.; Kuiper, D. L.; Scott, B. L.; Williams, U. J.; Kikkawa, J. M.; Schelter, E. J.; Boncella, J. M. *Inorg. Chem.* **2011**, *50*, 4235−4237.
(26) Zi, G.; Blosch, L. L.; Jia, L.; Andersen, R. A. *Organometallics* **2005**, *24*, 4602−4612.
(27) Stewart, J. L.; Andersen, R. A. *New J. Chem.* **1995**, *19*, 587−595.
(28) Diaconescu, P. L.; Arnold, P. L.; Baker, T. A.; Mindiola, D. J.; Cummins, C. C. *J. Am. Chem. Soc.* **2000**, *122*, 6108−6109.
(29) Vlaisavljevich, B.; Diaconescu, P. L.; Lukens, W. L.; Gagliardi, L.; Cummins, C. C. *Organometallics* **2013**, *32*, 1341−1352.
(30) Burns, C. J.; Smith, W. H.; Huffman, J. C.; Sattelberger, A. P. *J. Am. Chem. Soc.* **1990**, *112*, 3237−3239.
(31) Lewis, A. J.; Nakamaru-Ogiso, E.; Kikkawa, J. M.; Carroll, P. J.; Schelter, E. J. *Chem. Commun.* **2012**, *48*, 4977−4979.
(32) Lewis, A. J.; Carroll, P. J.; Schelter, E. J. *J. Am. Chem. Soc.* **2013**, *135*, 511−518.
(33) Lewis, A. J.; Carroll, P. J.; Schelter, E. J. *J. Am. Chem. Soc.* **2013**, *135*, 13185−13192.
(34) Guo, Y.-R.; Wu, Q.; Odoh, S. O.; Schreckenbach, G.; Pan, Q.-J. *Inorg. Chem.* **2013**, *52*, 9143−9152.
(35) Lam, O. P.; Franke, S. M.; Nakai, H.; Heinemann, F. W.; Hieringer, W.; Meyer, K. *Inorg. Chem.* **2012**, *51*, 6190−6199.
(36) Brennan, J. G.; Andersen, R. A. *J. Am. Chem. Soc.* **1985**, *107*, 514−516.
(37) Zalkin, A.; Brennan, J. G.; Andersen, R. A. *Acta Crystallogr., Sect. C: Cryst. Struct. Commun.* **1988**, *44*, 1553−1554.
(38) Arney, D. S. J.; Burns, C. J. *J. Am. Chem. Soc.* **1995**, *117*, 9448−9460.
(39) Castro-Rodríguez, I.; Nakai, H.; Meyer, K. *Angew. Chem., Int. Ed.* **2006**, *45*, 2389−2392.
(40) Matson, E. M.; Forrest, W. P.; Fanwick, P. E.; Bart, S. C. *Organometallics* **2013**, *32*, 1484−1492.
(41) Kraft, S. J.; Fanwick, P. E.; Bart, S. C. *Organometallics* **2013**, *32*, 3279−3285.
(42) Evans, W. J.; Montalvo, E.; Ziller, J. W.; DiPasquale, A. G.; Rheingold, A. L. *Inorg. Chem.* **2010**, *49*, 222−228.
(43) Zi, G.; Jia, L.; Werkema, E. L.; Walter, M. D.; Gottfriedsen, J. P.; Andersen, R. A. *Organometallics* **2005**, *24*, 4251−4264.
(44) Straub, T.; Frank, W.; Reiss, G. J.; Eisen, M. S. *J. Chem. Soc., Dalton Trans.* **1996**, 2541−2546.
(45) Straub, T.; Haskel, A.; Neyroud, T. G.; Kapon, M.; Botoshansky, M.; Eisen, M. S. *Organometallics* **2001**, *20*, 5017−5035.
(46) Stewart, J. L. *Tris(bis(trimethylsilyl)amido)uranium: Compounds with Tri-, Tetra-,and Penta-Valent Uranium*; LBL-25240, Lawrence Berkeley Lab.: Berkeley, CA, 1988.
(47) Graves, C. R.; Yang, P.; Kozimor, S. A.; Vaughn, A. E.; Clark, D. L.; Conradson, S. D.; Schelter, E. J.; Scott, B. L.; Thompson, J. D.; Hay, P. J.; Morris, D. E.; Kiplinger, J. L. *J. Am. Chem. Soc.* **2008**, *130*, 5272−5285.
(48) Graves, C. R.; Scott, B. L.; Morris, D. E.; Kiplinger, J. L. *J. Am. Chem. Soc.* **2007**, *129*, 11914−11915.
(49) Graves, C. R.; Scott, B. L.; Morris, D. E.; Kiplinger, J. L. *Organometallics* **2008**, *27*, 3335−3337.
(50) Dulong, F.; Pouessel, J.; Thuery, P.; Berthet, J.-C.; Ephritikhine, M.; Cantat, T. *Chem. Commun.* **2013**, *49*, 2412−2414.
(51) Burns, C. J.; Clark, D. L.; Donohoe, R. J.; Duval, P. B.; Scott, B. L.; Tait, C. D. *Inorg. Chem.* **2000**, *39*, 5464−5468.
(52) O'Grady, E.; Kaltsoyannis, N. *J. Chem. Soc., Dalton Trans.* **2002**, 1233−1239.
(53) Denning, R. G. *J. Phys. Chem. A* **2007**, *111*, 4125−4143.
(54) La Pierre, H. S.; Meyer, K. *Inorg. Chem.* **2013**, *52*, 529−539.
(55) Brown, J. L.; Fortier, S.; Wu, G.; Kaltsoyannis, N.; Hayton, T. W. *J. Am. Chem. Soc.* **2013**, *135*, 5352−5355.
(56) Kocienski, P. J. *Protecting Groups*; Georg Thieme Verlag: Stuttgart, Germany, 2005.
(57) Arnold, P. L.; Pécharman, A.-F.; Love, J. B. *Angew. Chem., Int. Ed.* **2011**, *50*, 9456−9458.
(58) Castro-Rodriguez, I.; Olsen, K.; Gantzel, P.; Meyer, K. *J. Am. Chem. Soc.* **2003**, *125*, 4565−4571.
(59) Arnold, P. L.; Turner, Z. R.; Kaltsoyannis, N.; Pelekanaki, P.; Bellabarba, R. M.; Tooze, R. P. *Chem.—Eur. J.* **2010**, *16*, 9623−9629.
(60) Smiles, D. E.; Wu, G.; Hayton, T. W. *J. Am. Chem. Soc.* **2014**, *136*, 96−99.
(61) Fortier, S.; Brown, J. L.; Kaltsoyannis, N.; Wu, G.; Hayton, T. W. *Inorg. Chem.* **2012**, *51*, 1625−1633.
(62) Bart, S. C.; Anthon, C.; Heinemann, F. W.; Bill, E.; Edelstein, N. M.; Meyer, K. *J. Am. Chem. Soc.* **2008**, *130*, 12536−12546.
(63) James, A. M.; Laxman, R. K.; Fronczek, F. R.; Maverick, A. W. *Inorg. Chem.* **1998**, *37*, 3785−3791.
(64) Roberts, B. P.; Winter, J. N. *J. Chem. Soc., Chem. Commun.* **1978**, 545−546.
(65) Arnold, P. L.; Hollis, E.; Nichol, G. S.; Love, J. B.; Griveau, J.-C.; Caciuffo, R.; Magnani, N.; Maron, L.; Castro, L.; Yahia, A.; Odoh, S. O.; Schreckenbach, G. *J. Am. Chem. Soc.* **2013**, *135*, 3841−3854.
(66) Jones, G. M.; Arnold, P. L.; Love, J. B. *Chem.—Eur. J.* **2013**, *19*, 10287−10294.
(67) Evans, W. J.; Davis, B. L. *Chem. Rev.* **2002**, *102*, 2119−2136.
(68) Pennington, D. A.; Horton, P. N.; Hursthouse, M. B.; Bochmann, M.; Lancaster, S. J. *Polyhedron* **2005**, *24*, 151−156.
(69) Tsurugi, H.; Nagae, H.; Mashima, K. *Chem. Commun.* **2011**, *47*, 5620−5622.
(70) Koppang, R. *J. Fluor. Chem.* **1977**, *9*, 449−459.
(71) Arnold, P. L.; Mansell, S. M.; Maron, L.; McKay, D. *Nat. Chem.* **2012**, *4*, 668−674.
(72) Odom, A. L.; Arnold, P. L.; Cummins, C. C. *J. Am. Chem. Soc.* **1998**, *120*, 5836−5837.
(73) Korobkov, I.; Gambarotta, S. *Inorg. Chem.* **2010**, *49*, 3409−3418.
(74) Lewis, A. J.; Williams, U. J.; Carroll, P. J.; Schelter, E. J. *Inorg. Chem.* **2013**, *52*, 7326−7328.
(75) Roussel, P.; Alcock, N. W.; Boaretto, R.; Kingsley, A. J.; Munslow, I. J.; Sanders, C. J.; Scott, P. *Inorg. Chem.* **1999**, *38*, 3651−3656.
(76) Shannon, R. D. *Acta Crystallogr., Sect. A* **1976**, *32*, 751−767.
(77) Boaretto, R.; Roussel, P.; Kingsley, A. J.; Munslow, I. J.; Sanders, C. J.; Alcook, N. W.; Scott, P. *Chem. Commun.* **1999**, 1701−1702.
(78) Mills, D. P.; Moro, F.; McMaster, J.; van Slageren, J.; Lewis, W.; Blake, A. J.; Liddle, S. T. *Nat. Chem.* **2011**, *3*, 454−460.
(79) Potentials were determined from differential pulse voltammetry.
(80) Fortier, S.; Hayton, T. W. *Coord. Chem. Rev.* **2010**, *254*, 197−214.

(81) Barros, N.; Maynau, D.; Maron, L.; Eisenstein, O.; Zi, G.; Andersen, R. A. *Organometallics* **2007**, *26*, 5059−5065.
(82) Glendening, E. D.; Badenhoop, J. K.; Reed, A. E.; Carpenter, J. E.; Bohmann, J. A.; Morales, C. M.; Landis, C. R.; Weinhold, F. *NBO 6.0*; Theoretical Chemistry Institute, University of Wisconsin: Madison, WI, 2013.
(83) Schreckenbach, G.; Hay, P. J.; Martin, R. L. *Inorg. Chem.* **1998**, *37*, 4442−4451.
(84) PhB(MesIm) = phenyltris(1-mesitylimidazol-2-ylidene)borate.
(85) Scepaniak, J. J.; Young, J. A.; Bontchev, R. P.; Smith, J. M. *Angew. Chem., Int. Ed.* **2009**, *48*, 3158−3160.
(86) Thomson, R. K.; Cantat, T.; Scott, B. L.; Morris, D. E.; Batista, E. R.; Kiplinger, J. L. *Nat. Chem.* **2010**, *2*, 723−729.
(87) Matson, E. M.; Forrest, W. P.; Fanwick, P. E.; Bart, S. C. *Organometallics* **2012**, *31*, 4467−4473.
(88) Carmichael, C. D.; Jones, N. A.; Arnold, P. L. *Inorg. Chem.* **2008**, *47*, 8577−8579.
(89) Avens, L. R.; Bott, S. G.; Clark, D. L.; Sattelberger, A. P.; Watkin, J. G.; Zwick, B. D. *Inorg. Chem.* **1994**, *33*, 2248−2256.
(90) Yin, H.; Robinson, J. R.; Carroll, P. J.; Walsh, P. J.; Schelter, E. J. *Chem. Commun.* **2014**, *50*, 3470−3472.
(91) *SAINT*; Bruker AXS Inc.: Madison, WI, 2009.
(92) *SHELXTL*; Bruker AXS Inc.: Madison, WI, 2009.
(93) Sheldrick, G. M. *TWINABS*; University of Gottingen: Gottingen, Germany, 2008.
(94) Sheldrick, G. M. *SADABS*; University of Gottingen: Gottingen, Germany, 2007.
(95) Sheldrick, G. M. *Acta Crystallogr., Sect. A* **2008**, *64*, 112−122.
(96) Frisch, M. J.; Trucks, G. W.; Schlegel, H. B.; Scuseria, G. E.; Robb, M. A.; Cheeseman, J. R.; Scalmani, G.; Barone, V.; Mennucci, B.; Petersson, G. A.; Nakatsuji, H.; Caricato, M.; Li, X.; Hratchian, H. P.; Izmaylov, A. F.; Bloino, J.; Zheng, G.; Sonnenberg, J. L.; Hada, M.; Ehara, M.; Toyota, K.; Fukuda, R.; Hasegawa, J.; Ishida, M.; Nakajima, T.; Honda, Y.; Kitao, O.; Nakai, H.; Vreven, T.; Montgomery, J. A., Jr.; Peralta, J. E.; Ogliaro, F.; Bearpark, M.; Heyd, J. J.; Brothers, E.; Kudin, K. N.; Staroverov, V. N.; Kobayashi, R.; Normand, J.; Raghavachari, K.; Rendell, A.; Burant, J. C.; Iyengar, S. S.; Tomasi, J.; Cossi, M.; Rega, N.; Millam, N. J.; Klene, M.; Knox, J. E.; Cross, J. B.; Bakken, V.; Adamo, C.; Jaramillo, J.; Gomperts, R.; Stratmann, R. E.; Yazyev, O.; Austin, A. J.; Cammi, R.; Pomelli, C.; Ochterski, J. W.; Martin, R. L.; Morokuma, K.; Zakrzewski, V. G.; Voth, G. A.; Salvador, P.; Dannenberg, J. J.; Dapprich, S.; Daniels, A. D.; Farkas, Ö.; Foresman, J. B.; Ortiz, J. V.; Cioslowski, J.; Fox, D. J. *Gaussian 09*, revision D.01; Gaussian, Inc.: Wallingford, CT, 2009.
(97) Küchle, W.; Dolg, M.; Stoll, H.; Preuss, H. *J. Chem. Phys.* **1994**, *100*, 7535−7542.
(98) Cao, X.; Dolg, M. *J. Mol. Struct. (THEOCHEM)* **2004**, *673*, 203−209.
(99) Hehre, W. J.; Ditchfield, R.; Pople, J. A. *J. Chem. Phys.* **1972**, *56*, 2257−2261.

dx.doi.org/10.1021/ic501149u | *Inorg. Chem.* 2014, 53, 9129−9139